#### **ORGANIC CHEMISTRY**

# Visible light-mediated aza Paternò-Büchi reaction of acyclic oximes and alkenes to azetidines

Emily R. Wearing $^1$ , Yu-Cheng Yeh $^1$ , Gianmarco G. Terrones $^2$ †, Seren G. Parikh $^1$ †, Ilia Kevlishvili $^2$ , Heather J. Kulik $^2$ . $^3$ \*, Corinna S. Schindler $^1$ . $^4$ . $^5$ .6\*

The aza Paternò-Büchi reaction is a [2+2]-cycloaddition reaction between imines and alkenes that produces azetidines, four-membered nitrogen-containing heterocycles. Currently, successful examples rely primarily on either intramolecular variants or cyclic imine equivalents. To unlock the full synthetic potential of aza Paternò-Büchi reactions, it is essential to extend the reaction to acyclic imine equivalents. Here, we report that matching of the frontier molecular orbital energies of alkenes with those of acyclic oximes enables visible light-mediated aza Paternò-Büchi reactions through triplet energy transfer catalysis. The utility of this reaction is further showcased in the synthesis of epi-penaresidin B. Density functional theory computations reveal that a competition between the desired [2+2]-cycloaddition and alkene dimerization determines the success of the reaction. Frontier orbital energy matching between the reactive components lowers transition-state energy ( $\Delta G^{\ddagger}$ ) values and ultimately promotes reactivity.

oday, ~60% of all small-molecule drugs approved by the US Food and Drug Administration (FDA) incorporate at least one nitrogen-containing ring (1). Azetidines, four-membered N-heterocycles, are known to impart desirable properties, including increased three-dimensionality (2, 3), improved pharmacokinetics (4-7), and decreased lipophilicity (7). However, FDA-approved pharmaceuticals that incorporate azetidines remain underrepresented relative to their five- and six-membered counterparts and account for <1% of current medicines (8). This can in part be attributed to limited methods available for their construction (9-11), which hinders the incorporation of azetidines into pharmaceuticals and restrains development. A particular challenge is the synthesis of azetidines varied in the substitution of the 2- and 4-position, necessary to reach their full potential in current drug design (Fig. 1A). Thus, new methods to efficiently access azetidines are required to enable their application as improved functional handles in medicinal chemistry.

Traditionally, azetidines are accessed via nucleophilic substitution reactions of acyclic amines (10, 11), the reduction of  $\beta$ -lactams (12, 13), or strain-release substitution of azabicyclobutanes (Fig. 1A) (14). However, these approaches are limited and require harsh conditions or prefunctionalization of the starting material. Nucleophilic substitution approaches are restricted

<sup>1</sup>Department of Chemistry, University of Michigan, Ann Arbor, MI 48109, USA. <sup>2</sup>Department of Chemical Engineering, Massachusetts Institute of Technology, Cambridge, MA 02139, USA. <sup>3</sup>Department of Chemistry, Massachusetts Institute of Technology, Cambridge, MA 02139, USA. <sup>4</sup>Department of Chemistry, University of British Columbia, Vancouver V6T 121 BC, Canada. <sup>5</sup>Department of Biochemistry and Molecular Biology, University of British Columbia, Vancouver V6T 124 BC, Canada. <sup>6</sup>BC Cancer, Vancouver V5Z 1G1 BC, Canada.

\*Corresponding author. Email: hjkulik@mit.edu (H.J.K.); schindler@chem.ubc.ca (C.S.S.)

†These authors contributed equally to this work.

by the higher-energy conformational alignment required to achieve the reaction, with four-membered N-heterocycles being some of the most difficult to form (15). Select, highly substituted azetidines can be accessed through anionic ring closures; however, these require multistep synthetic sequences (16, 17). Although C-H activation (18–20) and hydrogen atom transfer-mediated approaches (21, 22) offer advancements in the construction of azetidine cores, more efficient and general approaches to directly access highly functionalized azetidines are still needed.

Arguably, the most direct approach to azetidines is the [2+2]-cycloaddition of imines and alkenes, known as the aza Paternò-Büchi reaction (23). Whereas [2+2]-cycloaddition reactions to form cyclobutanes (24, 25) and oxetanes (26, 27) have been well developed, the aza Paternò-Büchi reaction has remained limited because of challenges in capturing the imine excited state, which rapidly relaxes through isomerization, precluding cycloaddition (Fig. 1A) (23, 28, 29). Despite these limitations, visible light-mediated aza Paternò-Büchi reactions have attracted interest in recent years as atom-economical (30, 31) transformations to access highly functionalized azetidines (32-37). These methods are mediated by triplet energy transfer (EnT) from a photocatalyst and generally rely on two different approaches to overcome the challenges associated with imine isomerization: sensitization of an activated alkene [a conjugated alkene that can undergo energy transfer (e.g., a styrene or diene) (Fig. 1A)] (1), which can react intramolecularly with an unactivated oxime or hydrazone to form the azetidine product (32, 35, 38), or sensitization of an activated cyclic imine equivalent [a conjugated imine that can undergo energy transfer (e.g., isoxazoline, 2, 4)] that can undergo both intermolecular (4 + 3) (33, 36) and intramolecular (2) (34) cycloaddition with an unactiv Check for alkene. Nevertheless, none of these approaallow direct access to monocyclic azetidines, which requires the efficient conversion of acyclic imines with alkenes and thus represents a longstanding challenge (23). Only three examples of acyclic imines reacting in an intermolecular aza Paternò-Büchi reaction have been previously reported: a single example of an exocyclic imine reacting under ultraviolet irradiation (39); the cycloaddition of aryl sulfonyl imines and activated alkenes (40), which proceeds by a singlet-state exciplex mechanism; and the recently developed Cu-mediated cycloaddition of imines relying on copper-catalyzed activation of cyclic alkenes (41). In the case of the sulfonvl imine cycloaddition. the reaction proceeds through singlet excitation and the formation of an exciplex, which requires any substituents to enable  $\pi$ - $\pi$  stacking, limiting the scope (40). Although the newly developed copper-mediated methodology allows for the use of simple acyclic imines, cyclic alkene coupling partners remain a requirement, and monocyclic azetidines cannot be formed directly (41). Additionally, these approaches rely on ultraviolet light. The development of a visible light-mediated approach with acyclic substrates could greatly expand the scope and generality of this method.

To overcome this challenge, attempts were made to translate our previously developed methods using intramolecular cycloadditions of styrenes (1) (32) and intermolecular cycloadditions of cyclic isoxazolines (2 to 4) (33) with no success. We attributed this lack of reactivity to alternate relaxation pathways from the excited-state substrates, including imine isomerization (28, 29) and both isomerization and dimerization of styrenes (24, 42, 43) outcompeting the desired reaction path. We hypothesized that the limited reactivity of acyclic imines could be surmounted by matching the frontier orbital energies of the alkene and the oxime. Using two activated (conjugated) substrates, alkene 5 and oxime 6, facilitates improved frontier orbital energy matching as measured by  $\Delta E_{\rm FO}$  [ $\Delta E_{\rm FO}$  =  $E_{\rm oxime\ LUMO}$  – E<sub>alkene HSOMO</sub> (HSOMO, highest singly occupied molecular orbital; LUMO, lowest unoccupied molecular orbital)]. This matching of orbital energies results in lower transitionstate energy for the desired cycloaddition, ultimately enabling the formation of the desired azetidine products (7) (Fig. 1B).

### Reaction development

Our reaction design is centered on activated alkenes [e.g., styrenes (8) and dienes], on the basis of their triplet energy of  $\sim$ 60 kcal/mol (44), reactivity in EnT-mediated dimerization reactions (42, 43), and broad commercial availability. Simple glyoxylate oximes, which are activated by the conjugation of the oxime and ester group, were chosen as potential partners for

#### A Available synthetic strategies to access azetidines

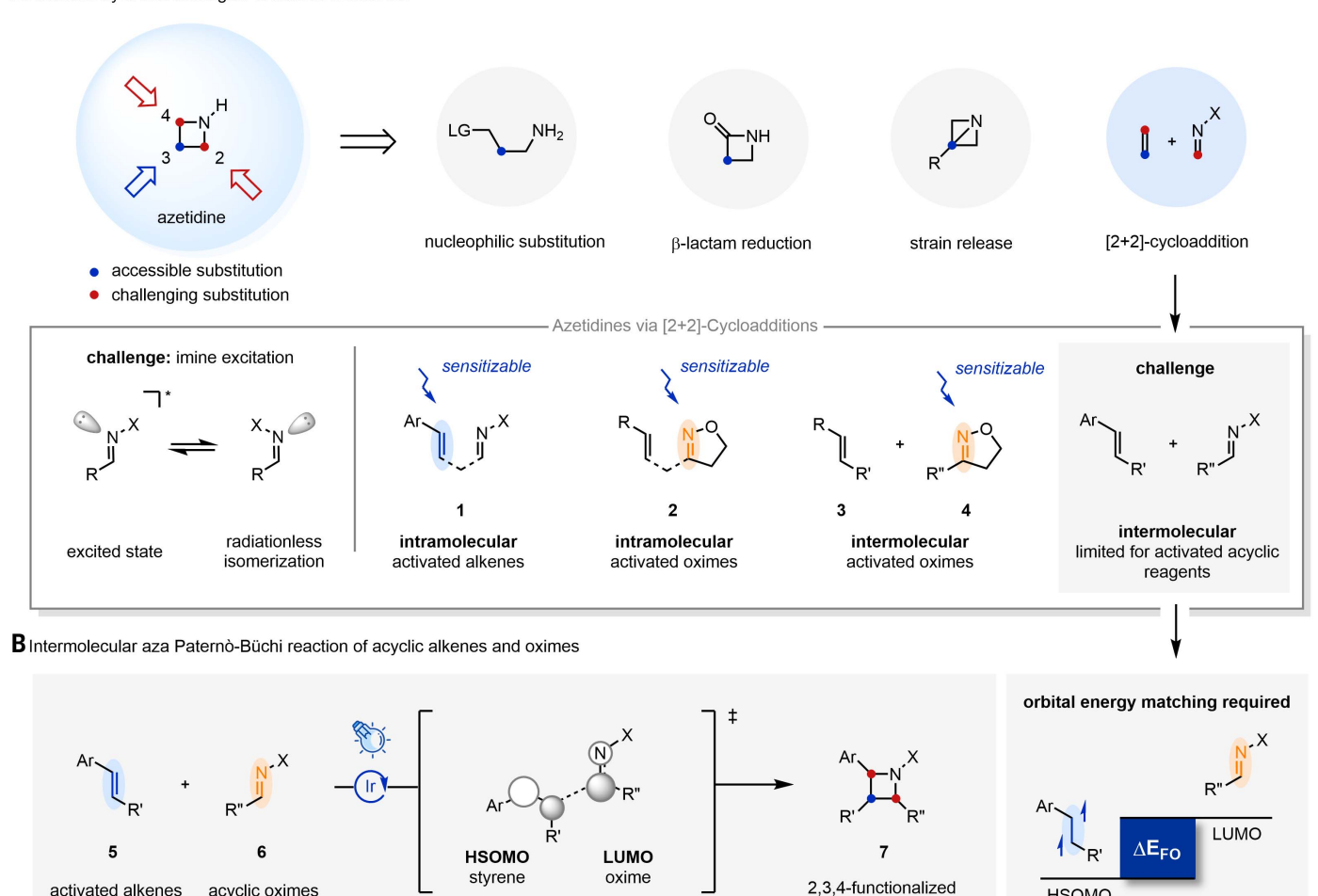


Fig. 1. Background and orbital alignment concept. (A) Traditional methods for azetidine synthesis include nucleophilic substitution, reduction of β-lactams, and strain release of azabicyclobutanes, which limits available substitution. The aza Paternò-Büchi reaction provides direct access to azetidines but is limited by imine isomerization. Approaches to overcome limitations to the

acyclic oximes

aza Paternò-Büchi reaction are restricted to cyclic imines or intramolecular reactivity. LG, leaving group. (B) This work describes the development of an intermolecular aza Paternò-Büchi reaction between two acyclic components which overcomes previous challenges by using activated starting materials which favor the desired cycloaddition reaction.

azetidines

нѕомо

the desired cycloaddition reaction. An initial evaluation revealed that upon sensitization with tris[3,5-difluoro-2-(2-pyridinyl)phenyl]-iridium [Ir(dFppy)<sub>3</sub>] as the photocatalyst, styrene 8 and oxime 9 were able to undergo the desired transformation providing azetidine 11 in 12% yield as a mixture of diastereomers (Fig. 2). However, optimization proved challenging, leading us to use a design of experiments (DOE) statistical approach (see supplementary materials for details). Using a two-factor (concentration, styrene loading), two-level experimental design including center points, we found that both oxime concentration and styrene loading had a statistically significant impact on yield (Fig. 2). On the basis of these results, raising both the oxime concentration and the styrene loading in consecutive additions enabled the formation of the azetidine product 12 in 83% yield (67% isolated).

A variety of styrenes, including electronneutral (11 and 12), electron-donating (13 to 16), and electron-withdrawing (17 to 19 and 23) examples, are all compatible with the optimal reaction conditions, with para-methoxy (13 and 14) and ortho-methoxy (16) groups providing the highest yields of up to 80% (Fig. 3). Alkenes with an extended  $\pi$ -system are also compatible (22), and heteroaryl alkenes (30 and 31) react to form the desired product in up to 55% yield. These heteroaryl groups such as pyridine (30) are highly desirable for drug discovery applications. Whereas the monosubstituted alkenes provide azetidines with substitution in the desired 2- and 4-positions, 1,1-disubstituted (21) and 1,2-disubstituted (20) alkenes also react to form the corresponding azetidine products. The yield of 21 could be improved from 20 to 33% by a swap to hexafluoroisopropanol (HFIP) as solvent (see supplementary materials for details). HFIP has previously been shown to increase yields in triplet-state cycloaddition reactions through substrate activation by H-bonding (45, 46). Trisubstituted alkenes form the products 24 and 25, resulting in desirable spirocyclic structures. These compounds were isolated in high diastereomeric ratios (d.r.), likely due to a combination of increased steric bulk on the alkene and challenges with isolation of the minor stereoisomer. Additionally, the lower yields in these cases are likely a result of steric effects also observed for tetrasubstituted alkenes, for which the reaction did not proceed. Conjugated dienes are also amenable to this transformation, as they have a similar triplet energy to styrenes (~60 kcal/mol), and provide **26**, **27**, and **29** as azetidines with an additional terminal alkene functional handle. Azetidines 26 and 27 were each isolated as a single regioisomer and

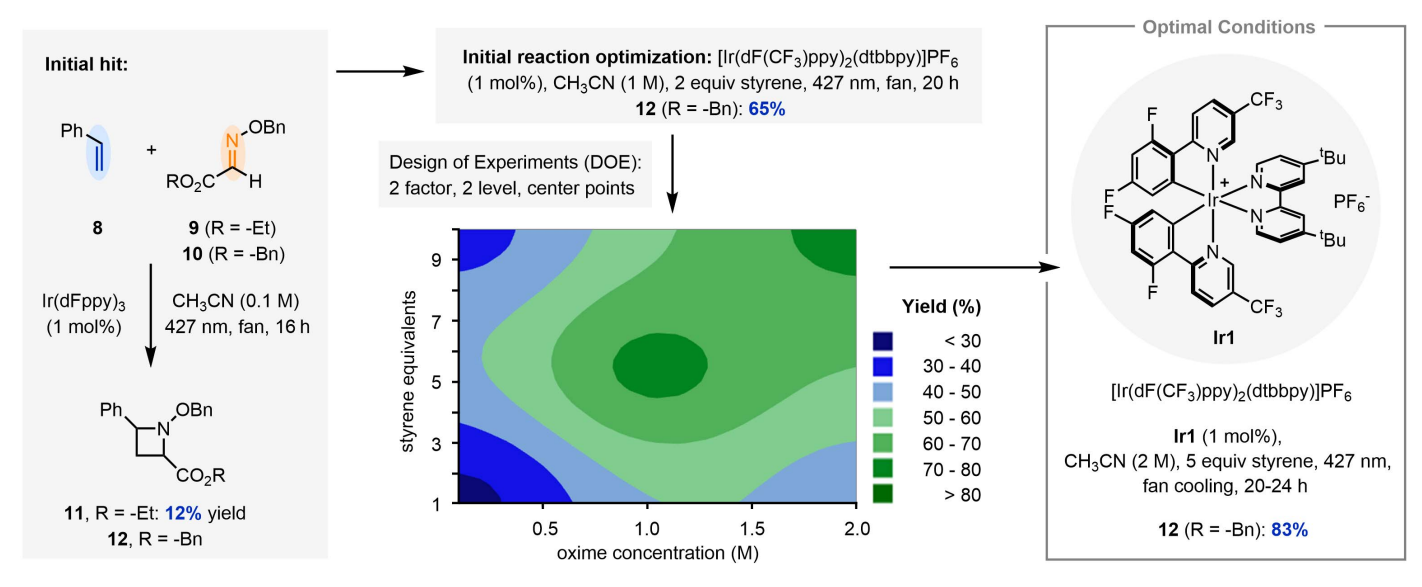


**Fig. 2. Initial hit and subsequent optimization.** A two-factor, two-level DOE approach was used to analyze the impact of styrene loading and oxime concentration (molarity is reported with respect to oxime starting material). Both factors were found to have a significant effect on yield (supplementary materials). Final optimization resulted in an improved yield of 83% (measured by <sup>1</sup>H NMR). Bn, benzyl; Bu, butyl; Et, ethyl; Ph, phenyl.

diastereoisomer, demonstrating the utility of this method in accessing 2,3,4-trisubstituted azetidines from asymmetric dienes with good regioselectivity. Oximes with both electronwithdrawing (32 and 33) and electron-donating groups (35) on the oxime ester react comparably, with products 33 and 35 both forming in 70% yield. Benzyl and PMB esters were used to aid isolation of the azetidine products, and distinct esters react similarly in the transformation, providing 11 in 43% yield and 34 in 57% yield. Similarly, the oxime-protecting group was shown to have minimal impact with methyl- (33 to 35) and allyl-protected (36) oximes providing products in yields of 57 (34) to 70% (35). Whereas our previous visible lightmediated aza Paternò-Büchi approaches were limited to 2-isoxazoline esters and nitriles (33), products can be formed from oxime amides (37 to 40), including a Weinreb amide (39) and -NHcontaining amide (40) in up to 46% yield. Scaling the reaction from 0.25 to 2 mmol (13) enabled a drop to 3 equivalents of alkene, resulting in 61% yield. A limitation of this approach is that ketonederived oximes were not reactive. Because the mechanism of this transformation relies on bond formation between the styrene triplet biradical and the oxime as the rate-determining step, we hypothesize that the additional steric bulk around the oxime carbon prevents the desired reactivity (see "Mechanistic studies" below).

The optimal conditions are similarly applicable to cyclic alkenes generating bi- or tricyclic products in 19 to 99% yield (Fig. 4). Phenyl cyclohexene performs well in the reaction, which results in the quantitative formation of **43** and 94% yield of **44** as a single diastereomer, with the high yields in this case presumably arising from the longer triplet lifetime

of the cyclic triplet alkene. Furthermore, in this example, the additional steric bulk of the alkene disfavors competing alkene dimerization as evidenced by a lack of alkene dimer in the crude nuclear magnetic resonance (NMR) spectrum, enabling increased product formation. When scaled to 1 g (4 mmol), the reaction still performed well, providing 44 in 71% yield after purification of the product by recrystallization from the reaction mixture. To demonstrate the synthetic utility of this transformation in accessing free azetidines, 44 was reduced to the corresponding alcohol, which underwent N-O bond cleavage to form unprotected azetidine 45 or tosyl-protected azetidine 46 upon subsequent treatment with p-toluenesulfonyl chloride (TsCl). A six-membered diene also provides product 42 in 73% yield, and phenyl cyclobutene undergoes the reaction to form fused bicyclic system 47. Tricyclic systems can be generated through the reaction of fused bicyclic alkenes (48 to 52) with products being formed in 34 to 90% yield. Notably, N-methylmaleimide also reacts in this transformation forming 53, enabled by its comparable triplet energy to styrene (55.9 kcal/mol) (47). The formation of this product shows the versatility of this method beyond styrenes and dienes. The cyclic alkene substrates also reacted with amide-substituted oximes (54 and 55).

To explore the compatibility of this approach with substrates relevant to drug discovery, we performed the reaction with alkenes appended to biologically relevant molecules (Fig. 4). Reaction of **10** with an alkene derived from amoxapine, an antidepressant (48), formed **56** in 33% yield. Alkenes derived from vanillin, p-galactose, and indomethacin [a nonsteroidal anti-inflammatory pain reliever used to treat

arthritis (49)] performed similarly, yielding **58**, **59**, and **61**, respectively. Notably, both the aldehyde in **58** and the protected sugar in **59** are well tolerated, which indicates the utility of the mild photochemical conditions when applied to more complex substrates. Alkenes derived from the hormone estrone and natural product camphor both performed well, providing **57** and **60** in 72 and 69% yield, respectively, comparable to yields for simpler alkenes. The success of these substrates indicates the immediate applicability of this method to the complex compounds used in drug discovery applications.

Encouraged by the potential to acquire 2,3,4trifunctionalized azetidines through the [2+2]cycloaddition, we recognized that the azetidine core of natural products penaresidin A and B could be accessible. Originally isolated from the marine sponges Penares sp. (50), these sphingosine alkaloids are recognized for their biological activity as adenosine triphosphatase activators (51) and have shown cytotoxic effects against lung and colon tumor cells (52). Penaresidin A and B have been targets of 11 prior syntheses that have exclusively relied on nucleophilic substitution for azetidine formation (51, 53-63). Motivated to use our newly developed aza Paternò-Büchi reaction to synthesize derivatives of this valuable natural product, we initially prepared diene 64 from hydrogenation of 62 followed by elimination of the methoxy group in 63. Given that diene 64 incorporated the side chain functionalization of penaresidin B, we anticipated that [2+2]-cycloaddition with oxime 65 could provide access to the functionalized natural product core. As expected, the reaction of 64 with oxime 65 produced the corresponding azetidine product. After partial purification,

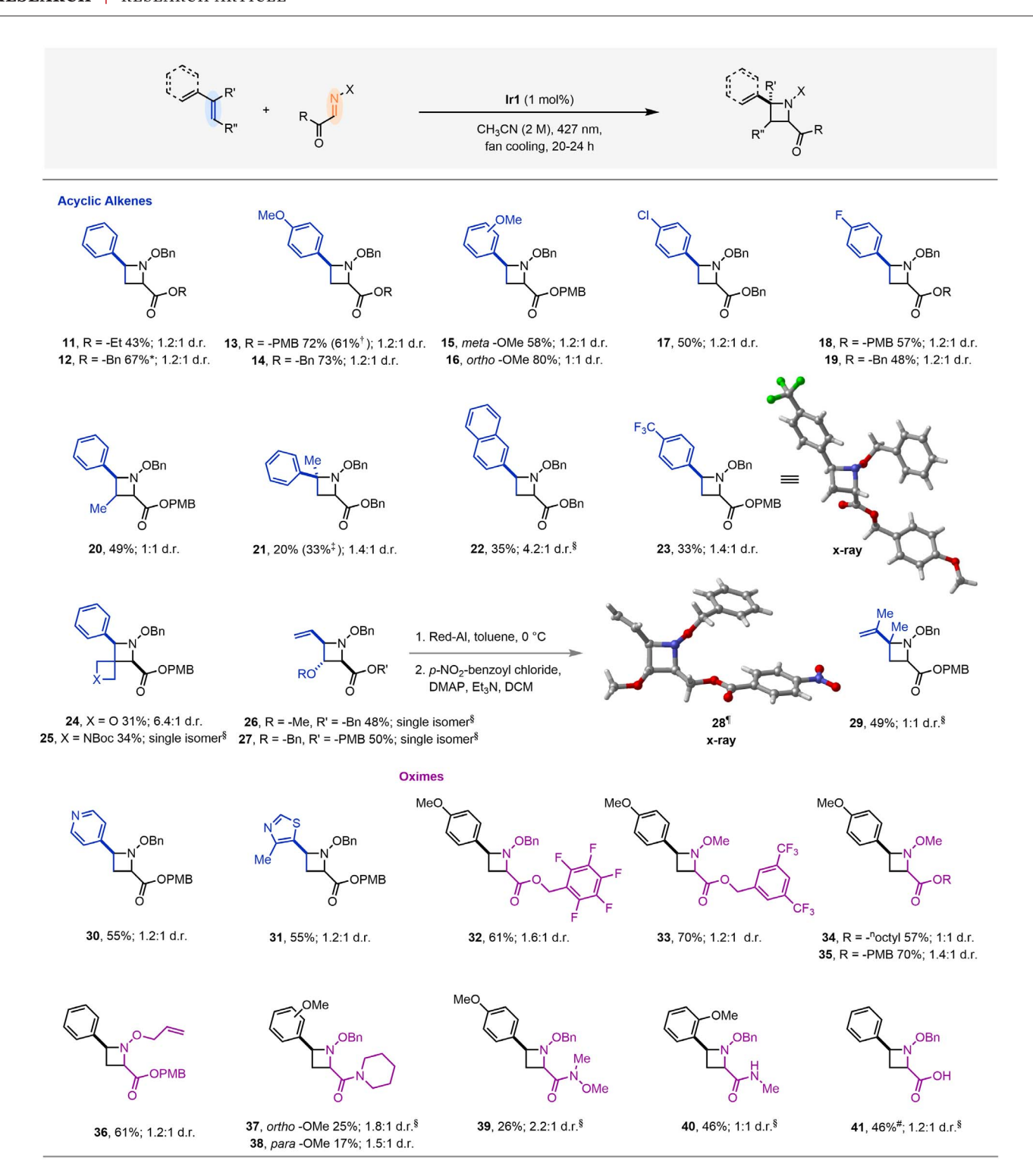


**Fig. 3. Substrate scope of acyclic alkenes and oximes.** 0.25 mmol oxime and **Ir1** (1 mol %) are added to a 1.5-dram vial with stir bar and dissolved in acetonitrile (2 M relative to oxime). The reaction mixture is sparged for 7 to 10 min, and alkene (0.625 mmol) is added. The reaction is irradiated with two blue light–emitting diode (LED) lamps (427 nm) and fan-cooled for 6 hours, at which point additional alkene (0.625 mmol) is added. The reaction is irradiated for an additional 14 to 18 hours for a total reaction time of 20 to 24 hours. For solid alkenes, one addition is made before sparging (1.25 mmol). Yields are reported of isolated product.

Diastereomeric ratios of the crude mixture are determined by <sup>1</sup>H NMR. Crystal for x-ray of **23** was grown after isolation of this diastereomer (minor diastereomer). \*0.15-mmol scale. †2-mmol scale, 3 equiv. alkene added over 6 hours, 0.25 mol% **Ir1**. ‡HFIP, 2 equiv. alkene, 465 nm light. §d.r. calculated from isolated material owing to overlap of peaks in <sup>1</sup>H NMR. ¶Treatment of **26** with Red-Al (60%), toluene, 0°C, 30 min. Product was isolated and then treated with *para*-nitrobenzoyl chloride, 4-(dimethylamino)pyridine (DMAP), Et<sub>3</sub>N, dichloromethane (DCM), for 2 hours to form **28**. #465 nm. -PMB, *para*-methoxybenzyl; Me, methyl; Boc, *tert*-butoxycarbonyl.

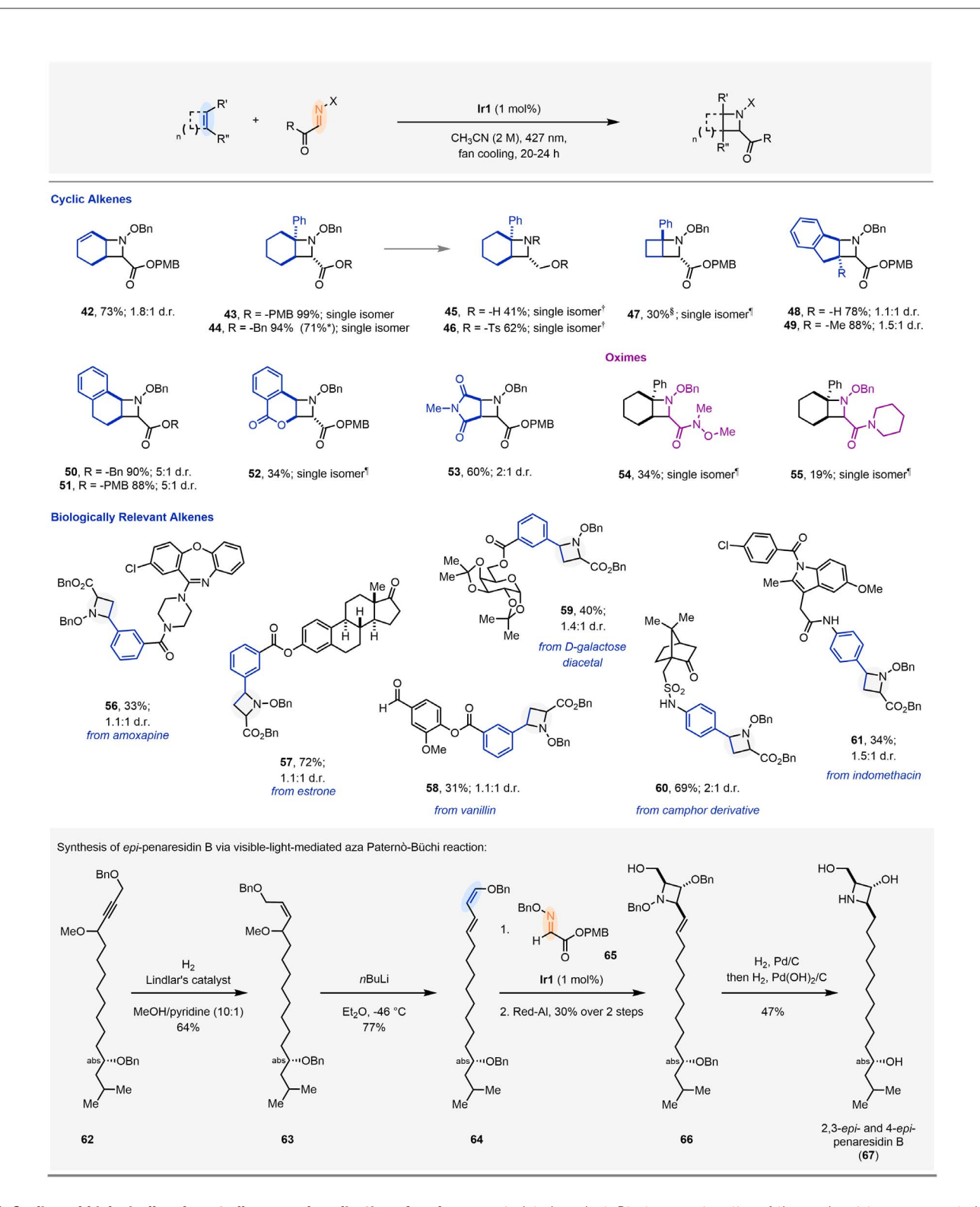


**Fig. 4. Cyclic and biologically relevant alkenes and application of cycloaddition to total synthesis.** For cyclic alkenes: 0.25 mmol oxime and **Ir1** (1 mol%) are added to a 1.5-dram vial with stir bar and dissolved in acetonitrile (2 M relative to limiting reagent). The reaction mixture is sparged for 7 to 10 min, and alkene (0.625 mmol) is added. The reaction is irradiated with fan-cooling with two blue LED lamps (427 nm) for 6 hours, at which point additional alkene (0.625 mmol) is added. The reaction is irradiated for an additional 14 to 18 hours for a total reaction time of 20 to 24 hours. For solid alkenes, one addition is made before sparging (1.25 mmol). Yields are reported of

isolated product. Diastereomeric ratios of the crude mixture are reported as determined by <sup>1</sup>H NMR. \*Run on a 1-g, 4-mmol scale with 3 equiv. alkene (added via syringe pump) and 0.25 mol % catalyst. †Ester reduction using Red-Al to form azetidine alcohol, then N–0 bond homolysis using Zn/HCl to form **45**. Protection with TsCl before isolation yields **46** (see supplementary materials for details). §Run on a 0.10-mmol scale with 2.3 equiv. alkene. ¶d.r. calculated from isolated material. For biologically relevant alkenes: run under the optimal conditions described in Fig. 2 with 2.5 equiv. oxime and 1 equiv. of alkene.

the azetidine product could be reduced with Red-Al [sodium bis(2-methoxyethoxy)aluminum hydride] to afford azetidine alcohol **66**. After a one-pot hydrogenation and global deprotection sequence, 2,3-epi- and 4-epi-penaresidin B (**67**) were obtained in 47% yield. Related penaresidin stereoisomers have recently been demonstrated to exhibit similar or improved cytotoxicity compared with the natural diastereomer (52). The successful synthesis of epi-penaresidin B (**67**) underscores the substantial advancements and synthetic applicability of this transformation.

#### **Mechanistic studies**

Subsequent efforts focused on a combination of experimental and theoretical investigations to understand how previous challenges associated with the photoreactivity of acyclic

imines were overcome. Initial electrochemical experiments showed that neither substrate would favorably undergo oxidation or reduction from the photocatalyst and were therefore consistent with an EnT mechanism (see supplementary materials for details). Ensuing endeavors centered on determining which substrate undergoes sensitization to its triplet state. As styrene 8 and oxime 10 are both activated, either could be sensitized by the catalyst (Fig. 5A). Indeed, analysis of the crude mixture revealed that styrene dimer 68 and isomerized oxime 69 are formed, which suggests that both can access their triplet states I1 and I2, respectively, under the optimal reaction conditions (Fig. 5A). Additional Stern-Volmer quenching experiments showed that styrene 8 has a much larger quenching constant ( $K_{SV} = 2.56 \text{ mM}^{-1}$ ) than oxime **10** ( $K_{SV} =$ 0.01 mM<sup>-1</sup>), consistent with a more favorable energy transfer event with the photocatalyst. This consideration combined with an excess of styrene 8 in the solution suggests that it is more likely for styrene to be sensitized to its triplet state  $\mathbf{\Pi}$  and initiate the desired cycloaddition with oxime 10. Control reactions between activated and unactivated pairings of substrates further corroborate the hypothesis that the styrene triplet state **I1** is primarily responsible for the observed reactivity (Fig. 5, B and C). Specifically, styrene 8 forms trace amounts of azetidine product 71, observed by mass spectrometry analysis and <sup>1</sup>H NMR when paired with unactivated oxime 70, whereas activated oxime 10 forms no products, as seen by mass spectrometry analysis, with unactivated alkene

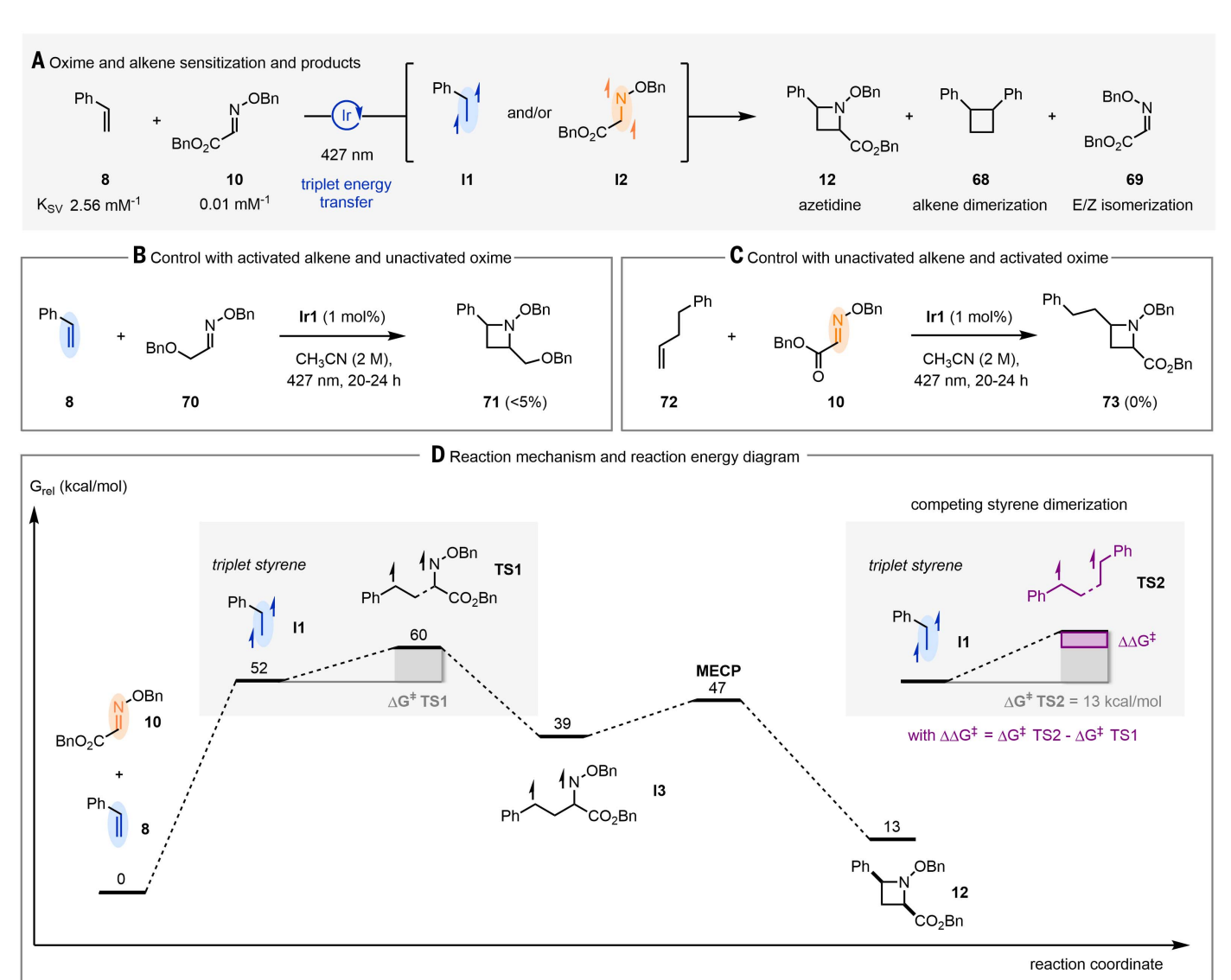
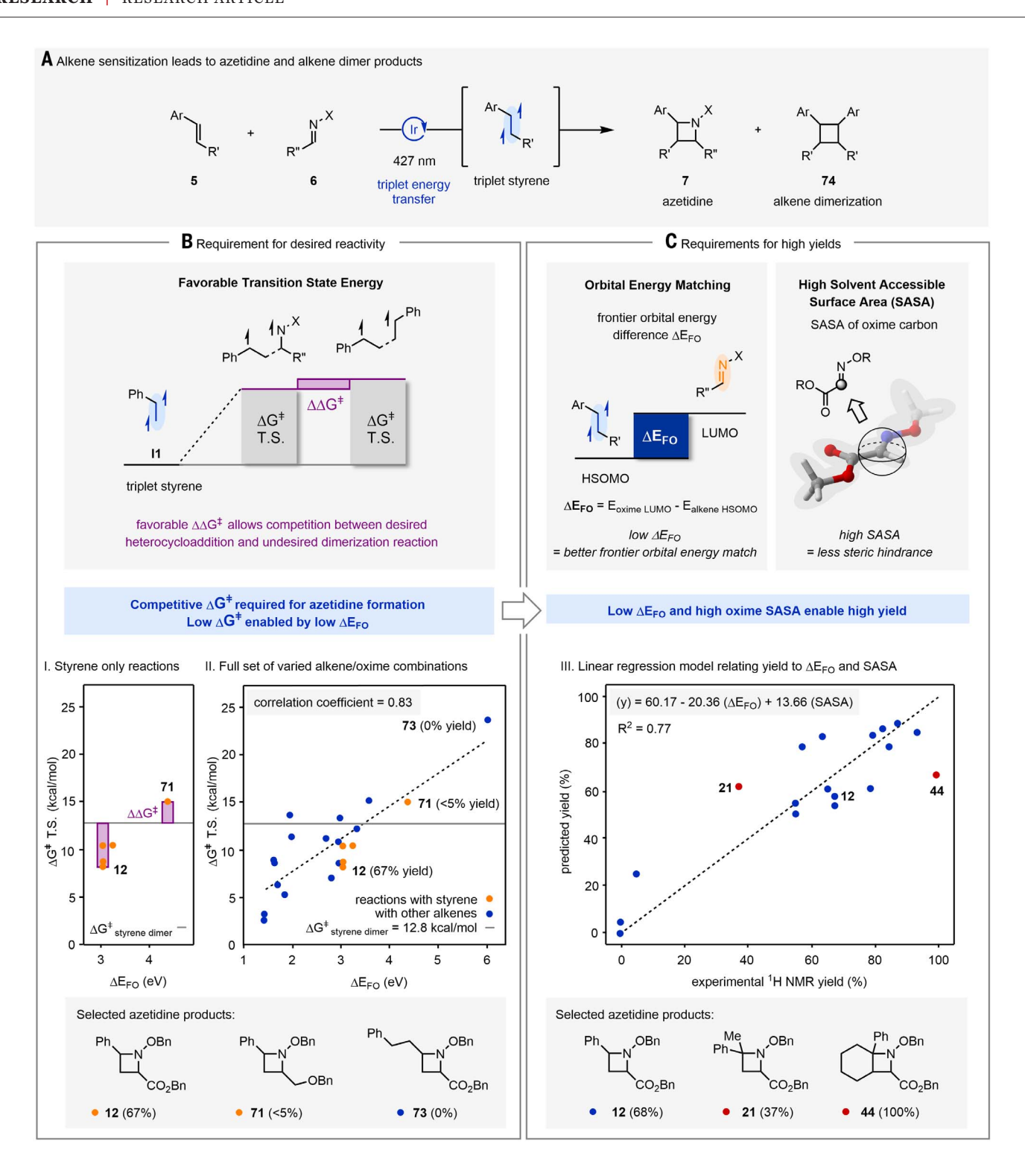


Fig. 5. Mechanistic studies. (A) Based on the observed byproducts of the reaction, both triplet-state styrene and oxime are accessible. Stern–Volmer quenching studies show styrene is more readily sensitized to its triplet state by Ir1. (B and C) Control reactions pairing an unactivated oxime with an activated alkene (B) and an unactivated alkene with an activated oxime (C). (D) DFT-computed energy diagram for the formation of 12 and comparison of the desired azetidine formation with styrene dimerization. MECP, minimum energy crossing point, transition from triplet to singlet state.



**Fig. 6. Factors underlying efficient cycloaddition reactivity.** (**A**) General scheme for this [2+2]-cycloaddition with two activated components resulting in azetidine and alkene dimer. (**B**) For productive azetidine formation, the transition-state (T.S.) free energy ( $\Delta G^{\ddagger}$ ) for the desired reaction must be lower than or comparable to  $\Delta G^{\ddagger}$  for styrene dimerization. Comparison of  $\Delta G^{\ddagger}$  with a measure of the frontier orbital energy match of the two components ( $\Delta E_{FO}$ ) shows a strong correlation, with high  $\Delta E_{FO}$  leading to higher  $\Delta G^{\ddagger}$  (plot II, dashed line is best-fit line). Reactions with styrene are highlighted as orange points and

can be compared to the styrene dimerization  $\Delta G^{\ddagger}$  (plot I). Comparing the transition-state energy for the productive reactions with the unproductive activated-unactivated pairing (71) explains the observed reactivity. (C) Linear regression model for predicting  $^1H$  NMR yield based on  $\Delta E_{FO}$  and oxime SASA demonstrates that better frontier orbital energy matching (low  $\Delta E_{FO}$ ) and decreased oxime steric hindrance (high oxime SASA) promote higher yields (plot III, dashed line is parity line). High error points are shown in red.  $^1H$  NMR yields shown for labeled points.

72 under otherwise identical reaction conditions (see below for further discussion). On the basis of these results, the following mechanism for the reaction is proposed: First, styrene 8 is sensitized by the photocatalyst to its triplet state II, which then combines with the ground state of oxime 10 to form triplet 1,4-biradical 13. This biradical then undergoes intersystem crossing between the excited triplet- and groundstate singlet energy surface through the minimum energy crossing point and spontaneous ring closing to form the azetidine product 12. The density functional theory (DFT)-computed energy surface for this reaction indicates that the rate-determining step is the initial combination of the triplet styrene and ground-state oxime to form the 1,4-biradical intermediate 13, through transition state TS1 (Fig. 5D; computational details in supplementary materials). Because styrene dimer 68 is observed in this transformation, the transition-state energy ( $\Delta G^{\dagger}$ ) for styrene dimerization (TS2) was also computed to be ~4.5 kcal/mol higher in energy  $(\Delta \Delta G^{\ddagger})$  than **TS1**. This is consistent with successful competition between formation of azetidine 12 and styrene dimerization to form 68.

Next, we sought to elucidate the features of the activated acyclic oximes that enable their previously elusive reactivity in [2+2]cycloadditions. We initially hypothesized that matching the frontier orbital energy levels of the alkene and acyclic oxime would result in favorable orbital interactions and ultimately promote reactivity. To test this hypothesis, we computationally investigated the relationship between  $(\Delta G^{\ddagger})$  and  $\Delta E_{\rm FO}$  (where  $\Delta E_{\rm FO}$  represents the difference in energy levels between the oxime LUMO and triplet-state alkene HSOMO, serving as a measure of frontier orbital energy matching;  $\Delta E_{\text{FO}} = E_{\text{oxime LUMO}} - E_{\text{alkene HSOMO}}$ across a variety of substrates (Fig. 6B; complete list of reactions analyzed in supplementary materials). To obtain these values, DFT calculations were performed by using the B3LYP functional (64-66), solvent, and dispersion corrections and a split valence basis for geometry optimization or a polarized triple-zeta basis for single-point calculations (see supplementary materials for details).

To investigate the criteria for effective substrate pairings, we examined a set of cycloadditions involving styrene (orange points in Fig. 6B, plot I). The reaction between styrene 8 and oxime 10, forming azetidine 12, exhibits a relatively low barrier of 8.3 kcal/mol, which enables it to compete with styrene dimerization (barrier of 12.8 kcal/mol, indicated with the gray line in Fig. 6B, plots I and II). By contrast, the reaction of unactivated oxime 70 with styrene 8, which forms azetidine 71, has a higher  $\Delta G^{\ddagger}$  (15.1 kcal/mol) that surpasses the  $\Delta G^{\ddagger}$  of styrene dimerization and hinders efficient azetidine formation, which instead leads primarily to the formation of dimer 68. Addi-

tionally, the  $\Delta E_{\rm FO}$  for this transformation is significantly higher than those of styrene 8 and activated oximes, such as 10. To assess the impact of  $\Delta E_{\rm FO}$  on  $\Delta G^{\ddagger}$  across a broader scope of reactions, these values were calculated for 21 selected azetidine products. A plot depicting  $\Delta G^{\dagger}$  versus  $\Delta E_{\rm FO}$  revealed a consistent trend across the dataset (Fig. 6B, plot II). Higher  $\Delta G^{\dagger}$ values are associated with larger  $\Delta E_{FO}$ , which demonstrates a clear relationship with a Pearson correlation coefficient of 0.83. This correlation underscores that reactions with substrates that feature closely matched orbital energies, reflected in lower  $\Delta E_{\rm FO}$  values, are more favorable. Furthermore, when considering the case of an activated oxime-unactivated alkene pairing (73), we observed the highest value of  $\Delta G^{\dagger}$  (23.7 kcal/mol) and  $\Delta E_{\rm FO}$  among all computationally analyzed reactions. This aligns with the absence of product formation in this transformation.

To determine what factors resulted in high vields, we examined 18 azetidines spanning the range of observed yields. Crude reaction yields were obtained by <sup>1</sup>H NMR, minimizing noise associated with product isolation. The dataset included computed values for  $\Delta E_{\rm FO}$  and oxime carbon solvent-accessible surface area (SASA) for the selected pairings. Pearson correlation coefficients were calculated between each feature and the reaction NMR yield. Results showed strong correlations for both  $\Delta E_{\rm FO}$  and oxime SASA with observed yield, indicated with correlation coefficients of -0.76 and 0.57, respectively. Furthermore,  $\Delta E_{\rm FO}$  and oxime SASA exhibited no correlation with each other, with a Pearson correlation coefficient of -0.18 over the 18 reactions with NMR yields, and -0.06 over all 26 computationally analyzed reactions. On the basis of these results, we constructed a multiple linear regression model to predict reaction yield as a function of  $\Delta E_{\rm FO}$  and oxime SASA (Fig. 6C, plot III; model details in supplementary materials). The model achieved a coefficient of determination  $(R^2)$  of 0.77 and a mean absolute error of 11. Additionally, in leave-one-out cross-validation, the model demonstrated good generalization, with an average mean absolute error of 12.3 across 18 train-test splits. These performance metrics indicate that the model effectively predicted yields across most reactions. There are two high error points, 21 and 44, for which the alkenes are expected to have additional effects on the reaction not captured in the model, such as an increased triplet lifetime for the cyclic alkene (44) and increased steric hindrance for the disubstituted alkene (21). The reaction yield is influenced by both  $\Delta E_{\rm FO}$  and oxime SASA as seen from the equation  $y = 60.17 - 20.36(\Delta E_{FO}) + 13.66(SASA)$ , in which higher  $\Delta E_{\rm FO}$  contributes to lower reaction yields, whereas increased oxime SASA correlates with higher yields. The impact of both factors aligns with the proposed mechanism,

demonstrating that the rate-determining step, the formation of the C–C bond between the oxime and the alkene, is made more favorable by improved orbital energy matching for these components (low  $\Delta E_{\rm FO}$ ) and decreased steric hindrance on the oxime carbon (high oxime SASA). This model also elucidates the limitations of this transformation concerning unactivated components and ketone-derived oximes, as unactivated components result in pairings with high  $\Delta E_{\rm FO}$  values, and ketone-derived oximes have increased steric hindrance at the oxime carbon, leading to smaller oxime SASA.

Taken together, these studies provide insight into which factors enable the previously inaccessible intermolecular reactivity between acyclic oximes and alkenes and which factors lead to high yields for this transformation (Fig. 6, B and C). Overall, these results suggest that two requirements must be fulfilled to allow for the intermolecular aza Paternò-Büchi reaction of acyclic oximes and alkenes to proceed: (i) the transition-state energy  $\Delta G^{\ddagger}$  must be low enough to compete with alkene dimerization, which is enabled by (ii) well-matched frontier orbital energies of the oxime and alkene substrate, as evidenced by a small frontier orbital energy difference  $\Delta E_{\rm EO}$ . These two requirements are fulfilled for activated oxime-alkene pairs but are not met by pairs involving unactivated oximes or alkenes; consequently, the unactivated substrates are not reactive in this transformation. Yields of this transformation are influenced by frontier orbital energy matching and the accessibility of the oxime carbon, with better-matched orbital energies and less sterically hindered oximes leading to higher yields overall. We expect that the results described here will have a direct impact on future [2+2]-cycloadditions of challenging substrates relying on the reactivity of triplet excited states.

Insights gained through the investigation of this transformation are expected to have implications for the further development of not only aza Paternò-Büchi reactions but all visible light-mediated [2+2]-cycloadditions using the styrene triplet state, which have historically been limited primarily to dimerization-type reactions. The demonstration of the importance of frontier orbital energy matching in enabling alkene-oxime cycloaddition to compete with alkene dimerization and form the desired product is an essential advancement in our understanding that will facilitate future cycloadditions beyond those of oximes and alkenes.

#### REFERENCES AND NOTES

- E. Vitaku, D. T. Smith, J. T. Njardarson, J. Med. Chem. 57, 10257–10274 (2014).
- F. Lovering, J. Bikker, C. Humblet, J. Med. Chem. 52, 6752–6756 (2009).
- F. Lovering, MedChemComm 4, 515-519 (2013).
- 4. A. Brown et al., Bioorg. Med. Chem. Lett. 20, 516-520 (2010).
- P. V. Fish, A. D. Brown, E. Evrard, L. R. Roberts, *Bioorg. Med. Chem. Lett.* 19, 1871–1875 (2009).
- 6. J. T. Lowe et al., J. Org. Chem. 77, 7187-7211 (2012).

- D. J. St Jean Jr., C. Fotsch, J. Med. Chem. 55, 6002–6020 (2012).
- On the basis of the number of currently approved azetidinecontaining drugs and total number of FDA-approved drugs (>19,000), of which ~60% are reported to contain an N-heterocycle.
- D. Antermite, L. Degennaro, R. Luisi, Org. Biomol. Chem. 15, 34–50 (2016).
- A. Brandi, S. Cicchi, F. M. Cordero, *Chem. Rev.* **108**, 3988–4035 (2008).
- 11. N. H. Cromwell, B. Phillips, Chem. Rev. 79, 331-358 (1979).
- 12. C. R. Pitts, T. Lectka, Chem. Rev. 114, 7930-7953 (2014).
- B. Alcaide, P. Almendros, C. Aragoncillo, *Chem. Rev.* 107, 4437–4492 (2007).
- M. Andresini, L. Degennaro, R. Luisi, Org. Biomol. Chem. 18, 5798–5810 (2020).
- J. Clayden, N. Greeves, S. Warren, in Organic Chemistry (Oxford Univ. Press, ed. 2, 2012), pp. 805–807.
- F. Couty, G. Evano, N. Rabasso, *Tetrahedron Asymmetry* 14, 2407–2412 (2003).
- P. Quinodoz, B. Drouillat, K. Wright, J. Marrot, F. Couty, J. Org. Chem. 81, 2899–2910 (2016).
- G. He, Y. Zhao, S. Zhang, C. Lu, G. Chen, J. Am. Chem. Soc. 134, 3-6 (2012).
- K. N. Betz, N. D. Chiappini, J. Du Bois, *Org. Lett.* 22, 1687–1691 (2020).
- M. Nappi, C. He, W. G. Whitehurst, B. G. N. Chappell,
  M. J. Gaunt, Angew. Chem. Int. Ed. 57, 3178–3182 (2018).
- 21. A. Osato, T. Fujihara, H. Shigehisa, *ACS Catal.* **13**, 4101–4110 (2023)
- 22. S. H. Park et al., J. Am. Chem. Soc. 145, 15360-15369 (2023).
- A. D. Richardson, M. R. Becker, C. S. Schindler, *Chem. Sci.* 11, 7553–7561 (2020).
- S. Poplata, A. Tröster, Y.-Q. Zou, T. Bach, Chem. Rev. 116, 9748–9815 (2016).
- D. Sarkar, N. Bera, S. Ghosh, Eur. J. Org. Chem. 2020, 1310–1326 (2020).
- M. D'Auria, Photochem. Photobiol. Sci. 18, 2297–2362 (2019).
- 27. M. D'Auria, R. Racioppi, *Molecules* 18, 11384-11428 (2013).
- 28. S. K. Kandappa, L. K. Valloli, S. Ahuja, J. Parthiban, J. Sivaguru, Chem. Soc. Rev. 50, 1617–1641 (2021)
- 29. A. C. Pratt, Chem. Soc. Rev. 6, 63-81 (1977)
- 30. B. M. Trost, Science 254, 1471-1477 (1991).
- 31. B. M. Trost, Acc. Chem. Res. **35**, 695–705 (2002).
- M. R. Becker, A. D. Richardson, C. S. Schindler, *Nat. Commun.* 10, 5095 (2019).
- M. R. Becker, E. R. Wearing, C. S. Schindler, *Nat. Chem.* 12, 898–905 (2020).
- D. E. Blackmun, S. A. Chamness, C. S. Schindler, Org. Lett. 24, 3053–3057 (2022).
- M. Zhu, X. Zhang, C. Zheng, S.-L. You, ACS Catal. 10, 12618–12626 (2020).

- W. Wang, M. K. Brown, Angew. Chem. Int. Ed. 62, e202305622 (2023).
- 37. X. Huang et al., J. Am. Chem. Soc. 139, 9120-9123 (2017).
- E. Kumarasamy, S. K. Kandappa, R. Raghunathan, S. Jockusch, J. Sivaguru, Angew. Chem. Int. Ed. 56, 7056–7061 (2017).
- P. Margaretha, *Helv. Chim. Acta* **61**, 1025–1032 (1978).
  R. Sakamoto, T. Inada, S. Sakurai, K. Maruoka, *Org. Lett.* **18**,
- 6252–6255 (2016).
  D. M. Flores, M. L. Neville, V. A. Schmidt, Nat. Commun. 13, 2764 (2022).
- 42. M. Golfmann, L. Glagow, A. Giakoumidakis, C. Golz, J. C. L. Walker, *Chemistry* **29**, e202202373 (2023).
- S. K. Pagire, A. Hossain, L. Traub, S. Kerres, O. Reiser, Chem. Commun. 53, 12072–12075 (2017).
- T. Ni, R. A. Caldwell, L. A. Melton, J. Am. Chem. Soc. 111, 457–464 (1989).
- 45. J. Ma et al., Science 371, 1338-1345 (2021).
- I. Triandafillidi, N. F. Nikitas, P. L. Gkizis, N. Spiliopoulou,
  C. G. Kokotos, *ChemSusChem* 15, e202102441 (2022).
- 47. S. Ha et al., Nat. Commun. 11, 2509 (2020).
- 48. R. B. Lydiard, A. J. Gelenberg, *Pharmacotherapy* **1**, 163–178 (1981).
- M. O'Brien, J. McCauley, E. Cohen, in Analytical Profiles of Drug Substances, vol. 13, K. Florey, Ed. (Academic Press, 1984), pp. 211–238, https://www.sciencedirect.com/science/ article/pii/S0099542808601926.
- J. Kobayashi et al., J. Chem. Soc., Perkin Trans. 1 1, 1135–1137 (1991).
- H. Yoda, T. Oguchi, K. Takabe, *Tetrahedron Lett.* 38, 3283–3284 (1997).
- 52. K. Ohshita et al., Bioorg. Med. Chem. 15, 4910-4916 (2007).
- 53. M. A. J. Dubois et al., J. Org. Chem. 88, 6476-6488 (2023).
- 54. S. M. Burns, T. J. McClure, S. G. Parikh, C. S. Schindler, Synthesis (Stuttg.) (2024).
- 55. T. Fujiwara et al., Tetrahedron 74, 4578-4591 (2018).
- F. Ding, R. William, S. M. Kock, M. L. Leow, X.-W. Liu, Chem. Commun. 51, 4639–4642 (2015).
- 57. H. Yoda, T. Uemura, K. Takabe, *Tetrahedron Lett.* **44**, 977–979 (2003)
- H. Takikawa, T. Maeda, M. Seki, H. Koshino, K. Mori, J. Chem. Soc., Perkin Trans. 1 1, 97–112 (1997).
- 59. S. Knapp, Y. Dong, Tetrahedron Lett. 38, 3813-3816 (1997).
- H. Takikawa, T. Maeda, K. Mori, Tetrahedron Lett. 36, 7689–7692 (1995).
- 61. D.-G. Liu, G.-Q. Lin, Tetrahedron Lett. 40, 337-340 (1999).
- 62. S. Raghavan, V. Krishnaiah, J. Org. Chem. 75, 748-761 (2010).
- B. V. S. Reddy, Ch. Kishore, A. S. Reddy, *Tetrahedron Lett.* 55, 49–51 (2014).
- 64. A. D. Becke, J. Chem. Phys. 98, 5648-5652 (1993).
- C. Lee, W. Yang, R. G. Parr, Phys. Rev. B Condens. Matter 37, 785–789 (1988).
- P. J. Stephens, F. J. Devlin, C. F. Chabalowski, M. J. Frisch, J. Phys. Chem. 98, 11623–11627 (1994).

 E. R. Wearing et al., Visible light mediated aza Paternò-Büchi reaction of acyclic oximes and alkenes to azetidines, Zenodo (2024); https://doi.org/10.5281/zenodo.10946528.

#### **ACKNOWLEDGMENTS**

We thank F. Qu for performing x-ray crystallography. Funding: This work was supported by the NSF Center for the Chemistry of Molecularly Optimized Networks (MONET; award CHE2116298) for personnel and the NIH (R01-GM141340) for the cost of chemicals and consumables. We thank the Alfred P. Sloan Foundation, the David and Lucile Packard Foundation, and the Camille and Henry Dreyfus Foundation for funding. E.R.W. thanks the NSF for a predoctoral fellowship (DGE-2241144) and The University of Michigan Rackham Graduate School for a predoctoral fellowship. This material is based on work supported by the National Science Foundation Graduate Research Fellowship Program (grant no. DGF-2241144). Any opinions, findings, and conclusions or recommendations expressed in this material are those of the author(s) and do not necessarily reflect the views of the National Science Foundation. This work used Expanse at the San Diego Supercomputer Center (SDSC) through allocation CHE140073 from the Advanced Cyberinfrastructure Coordination Ecosystem: Services & Support (ACCESS) program, which is supported by NSF grants 2138259, 2138286, 2138307, 2137603, and 2138296. Author contributions: E.R.W. and C.S.S. conceived the work. E.R.W., Y.-C.Y., and S.G.P. designed and performed experiments for the experimental work. G.G.T., I.K., and H.J.K. designed computational experiments, and G.G.T. and I.K. performed the computations. E.R.W., G.G.T., and C.S.S. prepared the initial manuscript draft, and all authors contributed to the final manuscript version. Competing interests: The authors declare no competing financial interests. Data and materials availability: The crystal structures presented in this work are available for free at the Cambridge Crystallographic Data Centre (CCDC) with deposition numbers 2280390 (anti-23) and 2280391 (28). Computational data are available through Zenodo (67). License information: Copyright © 2024 the authors, some rights reserved; exclusive licensee American Association for the Advancement of Science. No claim to original US government works. https://www. sciencemag.org/about/science-licenses-journal-article-reuse

## SUPPLEMENTARY MATERIALS

science.org/doi/10.1126/science.adj6771 Materials and Methods Supplementary Text Figs. S1 to S53 Tables S1 to S40 References (68–127) NMR Spectra

Submitted 10 July 2023; resubmitted 24 January 2024 Accepted 15 May 2024 10.1126/science.adi6771